RSC Advances

PAPER

View Article Online
View Journal | View Issue

Cite this: *RSC Adv.*, 2015, **5**, 35893

Bulk synthesis of highly conducting graphene oxide with long range ordering

Rachana Kumar,*[a] Samya Naqvi,[a] Neha Gupta,[a] Kumar Gaurav,[a] Saba Khan,[a] Pramod Kumar,*[b] Aniket Rana,[a] Rajiv K. Singh,[a] Ramil Bharadwaj[a] and Suresh Chand[a]

Received 31st January 2015
Accepted 13th April 2015

DOI: 10.1039/c5ra01943e

www.rsc.org/advances

Graphene oxide with high conductivity is today's demand not only for high quality graphene synthesis but also for direct applications in electronic devices. Here we demonstrate a milder bulk synthesis approach for graphene oxide (mGO) from tattered graphite showing long range ordering and much higher conductivity (27 S m^{-1}) compared to Hummers graphene oxide (H-GO) (0.8 S m^{-1}). A two step mild oxidation process is adapted instead of excessive oxidation of graphite based on Hummers method which creates permanent defects in carbon sheets. This work demonstrates the mild oxidation process for highly conducting GO preparation without use of $NaNO_3$ inhibiting the evolution of toxic gases and also possessing bulk synthesis possibilities.

Introduction

The two dimensional monolayer of carbon atoms, graphene, has found special commercial and academic research interest. Graphene possesses outstanding electrical, mechanical, thermal and optical properties,[1] while graphene derivatives like graphene oxide or other types of functionalized graphene have shown remarkable catalytic, mechanical, sensing and electronic properties offering a broad range of nanotechnological applications.[2] High quality graphene sheets with few defects are prepared by scotch-tape method and predominantly by chemical vapour deposition (CVD) but these methods are either complex or expensive.[3] However, graphene materials of different sheet size, functionalities and structures are widely prepared by cost effective chemical route through oxidation of graphite, *i.e.*, preparation of graphite oxide and further exfoliation to graphene oxide (GO).[4] In 1860, Brodie reported the oxidation of graphite to graphite oxide with $KClO_3$ and fuming HNO_3.[4a] Later on, Hummers and Offeman in 1958, developed a method for the synthesis of GO using H_2SO_4, $KMnO_4$ and $NaNO_3$.[4b] Hummer's process has several advantages over Brodie's approach but still having a few drawbacks like generation of toxic gases due to the use of $NaNO_3$, excessive oxidized and defective GO formation. Modified Hummer's processes have overcome a few disadvantages however, suffer from incomplete graphite to GO conversions.[5] Pre-oxidation of graphite with P_2O_5 and $K_2S_2O_8$ in H_2SO_4 could address the incomplete oxidation issue in Hummer's process but still possess several disadvantages like, low yield and poor quality due to extensive oxidation, small flake size and few layer graphene formation. Thus prepared Graphene oxide possess permanent defects, such as partial cleavage of hexagonal framework, producing low-quality graphene sheets on reduction and only partially restoring the structure and properties of graphene.[6] A wet chemical approach was reported to prepare graphene from GO with the carbon skeleton preserved in the order of tens of nanometers by controlled oxidation of graphite.[7] The use of $NaNO_3$ is also one of the concerns for large scale synthesis of GO due to release of toxic gases like NO_2 and N_2O_4 during oxidation.[8] Potassium permanganate ($KMnO_4$) in acidic media is one of the strongest oxidants resulting in complete intercalation of graphite with sulphuric acid without generation of any gases. *In situ* formed dimanganese heptoxide acts as oxidising agent[4d] and crucial is to control reaction temperature to avoid over-oxidation and formation of carbon dioxide preventing hole defects in graphene sheets.

In terms of electrical conductivity, highly oxidized graphene oxide is often considered as electrical insulator due to the disruption of sp^2 carbon network.[9] To recover the inherent electrical property of graphene sheets and to restore the honeycomb network, graphene oxide is reduced *via* several methods.[10] Although reduced GO (rGO) sheets are usually considered as one kind of chemically derived graphene, it is not appropriate to refer rGO as graphene sheets as there are still residual functional groups and defects resulting in substantially different properties.[6,11] It also has to be taken in account that once most of the oxygen groups are removed on reduction, rGO losses its dispersion capability due to increase in hydrophobicity and this is the biggest hurdle for their applications in devices where highly conducting material with least defects and solution processability is desirable. On the other hand, highly

[a]*Physics of Energy Harvesting Division, National Physical Laboratory, Dr. K. S. Krishnan Marg, New Delhi, 110012, India. E-mail: rachanak@nplindia.org*
[b]*Magnetic and Spintronic Laboratory, Indian Institute of Information Technology Allahabad, Uttar Pradesh, 211012, India. E-mail: pramod.phy@gmail.com*

conducting graphene oxide is required not only for graphene preparation but also for wide range applications.[2] The defects already present in graphene oxide produce poor quality graphene on reduction. Therefore, introduction of a milder oxidation process of graphite is the demand of today allowing low degree of oxidation preventing carbon frame rupture to obtain good quality graphene chemically.[12] Here we demonstrate the synthesis of low functionalized highly conducting graphene oxide (mGO) in bulk by mild chemical oxidation process preserving the carbon skeleton of the order of ~50 Å. We also prepared GO by modified Hummer's process (H-GO) to compare the properties with mGO. The advantage of the mild oxidation process for GO preparation is its simple approach, bulk synthesis possibilities, inhibition of toxic gas evolution and high conductive graphene oxide preparation.

To characterize the high quality of graphene oxide formed, we have used FTIR, UV-vis absorption, TGA, Raman spectroscopy, XRD and evaluated the electrical property by conductivity measurements. For the low degree of functionalization we used tattered graphite (t-graphite) as starting material[13] and mild oxidizing conditions to prepare mGO. Sulphuric acid and potassium permanganate were used for oxidation. Precautions have been taken during the addition of t-graphite–$KMnO_4$ slurry to sulphuric acid and an ice-bath is used to control the heat generated during reaction. This is important step to preserve the carbon framework. Product is collected by centrifugation and washed several times with water–methanol mixture to remove soluble impurities and obtained mGO, black in color than the usual brown colored H-GO. We have also rationalized the low degree of oxidation with $KMnO_4$–H_2SO_4 combination as oxidizing agent and proposed a mechanism.

Experimental section

Synthesis of H-GO (Scheme 1)

Micron sized graphite (1 g) and sodium nitrate (0.5 g) were dispersed in conc. sulphuric acid (25 mL) and potassium permanganate (3 g) was added over a period of 2 hours in ice cooled condition and stirred further for 2 hours at this temperature. 500 mL ice cooled DI water was added and 10 mL of 3% hydrogen peroxide was added very slowly with vigorous stirring while keeping the temperature ~0 °C. Graphite oxide was obtained by centrifugation and repeated washing till the supernatant obtained was neutral. Finally H-GO was yielded by ultrasonication (100 W). Yield: 430 mg.

Synthesis of mGO (Scheme 1)

Tattered graphite (t-graphite) was synthesized by refluxing micron sized graphite in conc. HNO_3 for 24 hours followed by washing with DI water and drying.[10] This t-graphite is used for graphene oxide preparation. In a typical reaction t-graphite (1 g) and potassium permanganate (3 g) are ground together until homogeneous. In a 250 mL beaker immersed in ice-bath, 30 mL 98% conc. sulphuric acid is taken and the above mixture is added pinch by pinch with continuous stirring over 30 minutes. After complete addition, ice bath is removed and stirring is continued at room temperature till the volumetric expansion is observed (~30 minutes). DI water (120 mL) is added again in ice bath with rapid stirring. The temperature of the bath is raised to 90 °C and stirred for 1 h. A homogenous black suspension is formed. The total suspension is centrifuged to discard the acidic supernatant and residue is washed several times (until pH was neutral) with water–methanol mixture to remove the soluble impurities. To fully exfoliate the GO sheets, the obtained residue is further suspended in water and ultrasonicated overnight (100 W) to get mGO. Yield: 410 mg.

Characterization techniques. Products were characterized using Fourier transform infrared spectroscopy (FTIR) using KBr pellets on Perkin Elmer FTIR Spectrum 2. FTIR spectra were collected over a range from 3500 to 500 cm^{-1}. A background spectrum in air was collected before scanning the samples. UV-vis spectroscopy measurement was performed on a Shimadzu UV-vis spectrophotometer in aqueous solution (1 mg/3 mL). Thermal gravimetric analysis (TGA) was run under nitrogen flow of 20 mL min^{-1} using Perkin Elmer (Pyris 1) TGA instrument and mass loss was recorded as a function of temperature. The samples were heated from room temperature to 900 °C at a ramp rate of 10 °C min^{-1}. Raman spectroscopy was performed on a Renishaw Raman Microscope in powder samples. Samples were also characterized by X-ray Diffraction

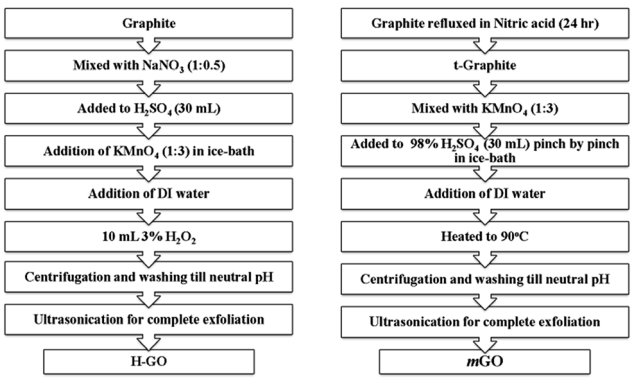

Scheme 1 Flow chart for synthesis of H-GO from graphite and mGO from t-graphite.

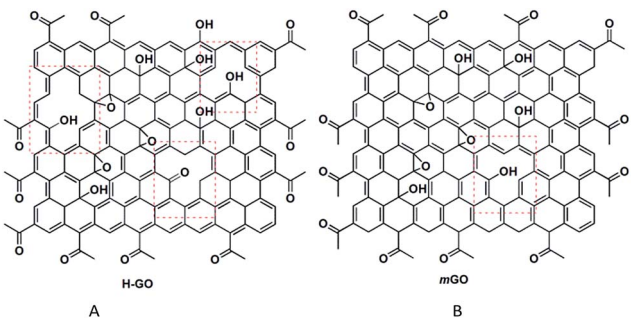

Fig. 1 Schematic of (A) highly defected (with holes) H-GO synthesized by modified Hummer's process and (B) controlled functionalized mGO with long range ordering and intact sp^2 carbon rings. Dotted rectangles show alkene sites for oxidation in graphene oxide synthesis.

on Rigaku diffractometer with Cu-Kα radiation ($l = 1.54056$ Å) to estimate the interlayer distances. SEM images were taken on a Zeiss EVO-MA10 scanning electron microscope and HRTEM analysis was done on Technai G^2 F30, HV-300.0 kV. The electrical conductivities were measured by four-point probe method using bottom contact patterned ITO by applying current source from High current source measurement unit (238) and reading voltage change from Keithley2000 multimeter at room temperature.

Results and discussion

In order to prepare graphene sheets with less defects and of reasonable quality from GO, much milder synthesis process is required by which C-atom rupture is prevented and preserving the sp^2 carbon skeleton (Fig. 1). Tattered graphite (t-graphite) is low functionalized graphite oxide with interlayer distance of 6.8 Å.[13] Second step of mild oxidation with sulphuric acid–potassium permanganate forms graphene oxide with less defects. According to classic Hummer's process, graphite with sodium nitrate is suspended in sulphuric acid and oxidized with potassium permanganate followed by addition of large amount of water and hydrogen peroxide. After vigorous washing process H-GO is obtained. In our process of mGO synthesis, we have avoided the use of sodium nitrate and also controlled the temperature during reaction to prevent the sp^2 C-network rupture. To avoid vigorous exothermic reaction, the homogeneous mixture of t-graphite and potassium permanganate is added to ice-cooled sulphuric acid with stirring. Addition of DI water was also done very slowly under ice cooled condition. Thus prepared mGO was easily collected by centrifugation and purified by washing with water : methanol mixture to remove acid and salt. The yield of the reaction was also reasonably good. 1 g of t-graphite yields ~410 mg of GO. Thus prepared black colored mGO is highly dispersible in water (2–3 mg mL^{-1}). The black color of mGO compared to usual brown color suspension of graphene oxide (H-GO), implies larger π-conjugated structure and stronger absorbance of visible light.

Combination of potassium permanganate and sulphuric acid is a common oxidizing agent and the active species is dimanganese heptoxide (Mn_2O_7).[4d] Tromel and Russ[14] had demonstrated that Mn_2O_7 selectively oxidizes the unsaturated aliphatic double bonds over aromatic bonds and this has direct implication in our oxidation process of t-graphite. If we apply their observation in our mild oxidation process, then the oxidation occurs on the isolated alkenes (defective sites already in t-graphite) rather than intact aromatic system (shown by dotted rectangles in Fig. 1). Mild oxidation of graphite for t-graphite preparation creates fewer defects and on further mild oxidation with $KMnO_4$–H_2SO_4, Mn_2O_7 species finds less number of aliphatic alkene sites and therefore less degree of oxidation is resulted in mGO keeping the long range ordering and honeycomb network (Fig. 1).

mGO and H-GO are characterized by FTIR, UV-vis, Raman spectroscopy, XRD, TEM and TGA analyses. FTIR clearly shows the functionalization of graphene sheets in both mGO and H-GO with O–H groups (3420 cm^{-1}) and C=O groups (1700 cm^{-1}). C=C stretching vibrations appear at 1620 cm^{-1} and C–O bond stretching is observed at 1250 cm^{-1}. The UV-vis absorption spectrum for same concentration of mGO and H-GO aqueous suspension is shown in Fig. 2. The UV-vis spectra of the two materials suggest that more ordered structure of mGO is due to the greater retention of carbon rings in basal plane compared to H-GO. The degree of conjugation or large aromatic regions can be determined by λ_{max} where higher conjugation means lesser energy is required for electronic transitions and high λ_{max} value is observed. mGO exhibits λ_{max} at 234 nm for π–π* transition of C=C and is 3 nm red-shift compared to H-GO (λ_{max} = 231 nm) along with hyperchromic effect. This suggests more number of aromatic rings retained for long range ordering. Both the materials show a similar shoulder at 300 nm for n–π* transition of carbonyl groups. UV-vis analysis also justifies the black color of mGO compared to brown color of H-GO due to higher absorbance.

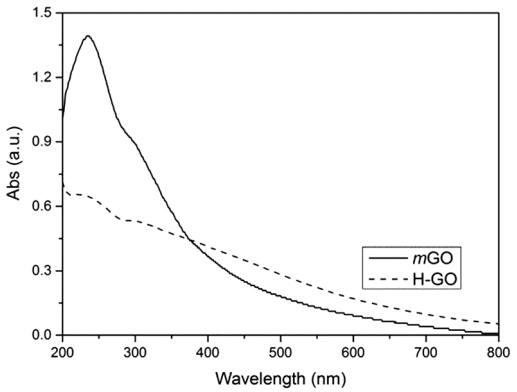

Fig. 2 UV-vis spectra of aqueous dispersion of mGO and H-GO (1 mg/3 mL). mGO showing red shifted π–π* transition band with higher absorbance.

There are only a few reports available where sodium nitrate and hydrogen peroxide are completely avoided from the GO synthesis process but have shown low λ_{max} value, high degree of oxidation and high weight loss in thermo gravimetric analysis (TGA).[7,15] To directly determine the degree of oxidation of mGO

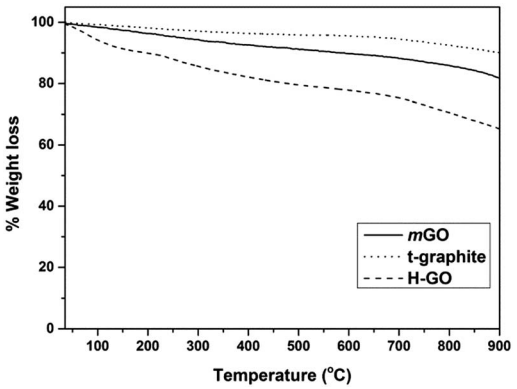

Fig. 3 TGA thermogram of t-graphite, mGO and H-GO under N_2 atmosphere.

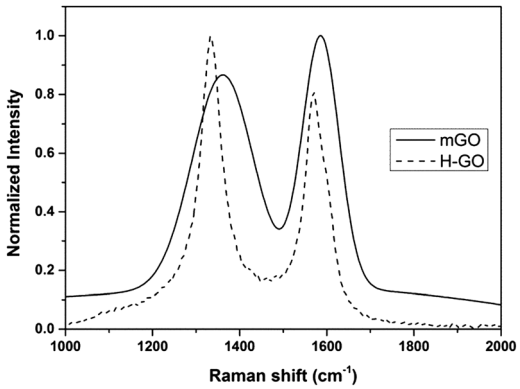

Fig. 4 Raman spectra of mGO and H-GO.

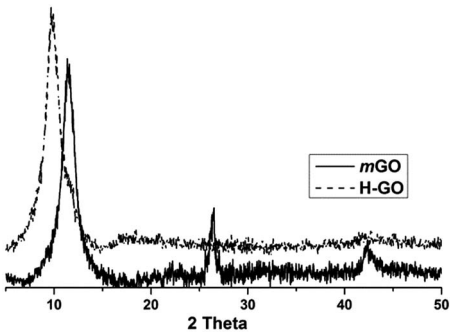

Fig. 5 Powder XRD of mGO and H-GO.

and H-GO, TGA was performed under N_2 atmosphere (Fig. 3).[16] Compared to 40% weight loss of H-GO, mGO shows only 23% weight loss up to 900 °C and 10% more than t-graphite directly ascertain the low functionalization in mGO. H-GO shows a ~10% weight loss below 200 °C resulting from the evaporation of adsorbed water and further 10% weight loss from 200 to 500 °C owing to the removal of the oxygen-containing functional groups. The weight loss of mGO is obviously lower than that of H-GO, especially between 200 to 500 °C, which demonstrates the decrease in the amount of oxygen-containing functional groups.

The two step oxidation has controlled the functionalization of graphene sheets while preserving its hexagonal framework is well evidenced by Raman spectroscopy (Fig. 4).[17] The defect induced D peak and G peak appear at 1359 and 1586 cm^{-1} respectively in mGO compared to H-GO at 1332 and 1572 cm^{-1} respectively. Huge red shifted peaks in mGO clearly signify the large domain size of sp^2 carbon rings. To further confirm the graphene like nature of mGO, we compared the I_D/I_G of mGO and H-GO as these ratios are usually used to evaluate the average size of sp^2 domains and defect density of GO.[18] mGO shows much reduced I_D/I_G ratio (0.85) compared to H-GO (1.2).

Even the reduced graphene oxide (rGO) prepared by various reducing agents show significantly increased I_D/I_G ratio which is attributed to the breakage of sp^3 C located hexatomic rings. As the G-band corresponds to the first order scattering of the E_{2g} mode related to the vibration of sp^2 bonded carbon atoms, while the D-band arises from the structural defects created by the attachment of oxygen groups on the carbon basal plane. Therefore the ratio of D/G band intensities is the measure of disorder and also considered as sp^3/sp^2 carbon ratio. In mGO small I_D/I_G ratio indicates much lower defect density and long range ordering of graphene sheets similar to chemically or thermally reduced GO (rGO).[19] We can further correlate it with the oxidation sites in t-graphite are only the already present defects (aliphatic alkene sites) and mild oxidation doesn't cause high bond breakage resulting in large sp^2 domains.

I_D/I_G is inversely proportional to average size of sp^2 domain or cluster diameter (L_α) calculated by Tuinstra and Koenig (TK) relationship[20] given by eqn (1)

$$I_D/I_G = C(\lambda)/L_\alpha \quad (1)$$

where $C(\lambda)$ is a constant dependent on laser intensity and equals to 44 Å for 515.5 nm laser used in Raman experiment. This equation is used for graphitic materials with domain size down to 20 Å and it is quite logical to apply this equation on mGO for cluster diameter calculation due to the less distortion of sp^2 carbon framework (low degree of sp^3 sites) compared to highly oxidized graphene oxide like H-GO as I_D/I_G is below 1. In mGO domain size (L_α) is calculated to be 51.1 Å (~20 sp^2 carbon rings) justifying our assumption of only aliphatic alkene sites oxidation in t-graphite for mGO formation.

The graphene like structure of mGO is also evidenced by X-ray diffraction (XRD) spectra. Fig. 5 shows the XRD pattern of mGO and H-GO. The calculated interlayer distance is proportional to degree of oxidation. The spacing for mGO and H-GO is calculated to be 7.82 Å and 9.0 Å respectively from the diffraction peak at 11.3° and 9.8° 2θ value for [001] plane of GO. H-GO shows larger interlayer distance than mGO which is attributed to higher degree of oxidation. Two more peaks appear at 26.4° and 42.3° for graphite like [002] plane and graphene [100] plane respectively in mGO. The reflection peak at 26.4° is attributed to the graphite like stretching of mGO sheets because of its large conjugated domain creating some chemically converted graphite regions (CCG). Crystallite size (D_p) was calculated using Scherer's equation. From GO [001] peak D_p was calculated to be 46 Å corroborating with Raman results.

TEM and SEM images of mGO are shown in Fig. 6 and 7 respectively. As is clearly seen, graphene oxide sheets of smooth several micron size were prepared by the two-step mild

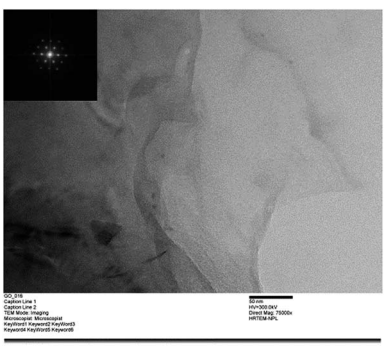

Fig. 6 TEM micrograph of mGO samples (FFT in inset).

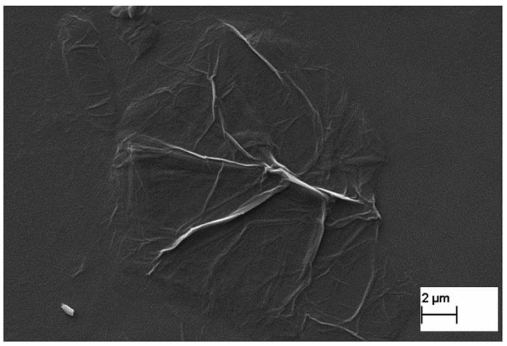

Fig. 7 SEM image of mGO showing several micron size graphene oxide sheet.

oxidation process and show sharp diffraction pattern suggesting more regular carbon framework than H-GO.[13a,15a] Finally to evident the preservation of inherent electrical property due to long range graphene like conjugated structure with less lattice disordering in mGO, we performed the electrical conductivity measurement and compared with H-GO. The conductivity of graphene oxide is dependent on the oxygen content and lattice defects.[21] Conductivity was measured by four-probe bottom contact patterned ITO device for both the samples (~75% optical transmittance at 300 nm). Electrodes (1 mm wide) were fabricated by laser patterning and scribing of ITO coated glass substrates of the size of 1 cm × 1 cm maintaining the spacing of 1 mm between the electrodes. Materials were coated by spin coating of aqueous suspensions (1 mg/2 mL) to obtain the films of 75% transmittance at 300 nm. A high impedance current source is used to supply current through the outer two probes, a voltameter is used to measure the voltage across the inner two probes. Bulk resistivity is calculated from *I–V* data using the eqn (2)

$$\rho_0 = 2a\pi sV/I \quad (2)$$

where, *s* is distance between the electrodes (0.1 cm) and the *a* is correction factor. Here the value of *a* is unity due to film thickness is much less than probe spacing.

The resistivity and thus the conductivity was calculated to be 27 S m^{-1} and 0.8 S m^{-1} for mGO and H-GO samples respectively. The conductivity measured for mGO is much higher than H-GO and also much higher than $NaBH_4$ reduced GO.[22] The high electrical conductivity of mGO also justifies the high sp^2 domain size (~51.1 Å) calculated by Raman experiment and high quality graphene oxide formation.

Conclusions

Improved synthesis methodology has been discussed for preparation of high quality graphene oxide and compared the properties with Hummer's GO (H-GO). The methodology avoids the evolution of toxic gases resulting in well dispersed mGO with regular framework structure showing high electrical conductivity compared to H-GO. In view of the above findings, synthesis of graphene oxide *via* two step mild oxidation process (mGO) envisages as a potential synthesis process for high quality graphene oxide for direct applications in energy storage devices, biomedical applications and for further production of high quality of graphene for electronic devices.

Acknowledgements

Authors acknowledge DST APEX program for funding.

Notes and references

1 M. J. Allen, V. C. Tung and R. B. Kaner, *Chem. Rev.*, 2010, **110**, 132–145.
2 (*a*) K. S. Mali, J. Greenwood, J. Adisoejoso, R. Phillipson and S. DeFeyter, *Nanoscale*, 2015, **7**, 1566–1585; (*b*) Y. Shen, Q. Fang and B. Chen, *Environ. Sci. Technol.*, 2015, **49**, 67–84; (*c*) J. Zhang, B. Guo, Y. Yang, W. Shen, Y. Wang, X. Zhou, H. Wu and S. Guo, *Carbon*, 2015, **84**, 469–478; (*d*) T. Liu, R. Kavian, I. Kim and S. W. Lee, *J. Phys. Chem. Lett.*, 2014, **5**, 4324–4330; (*e*) S. P. Dharupaneedi, R. V. Anjanapura, J. M. Han and T. M. Aminabhavi, *Ind. Eng. Chem. Res.*, 2014, **53**, 14474–14484; (*f*) D. P. Suhas, A. V. Raghu, H. M. Jeong and T. M. Aminabhavi, *RSC Adv.*, 2013, **3**, 17120–17130; (*g*) J. Liu, J. Tang and J. J. Gooding, *J. Mater. Chem.*, 2012, **22**, 12435–12452.
3 (*a*) K. S. Novoselov, A. K. Geim, S. V. Morozov, D. Jiang, Y. Zhang, S. V. Dubonos, I. V. Grigorieva and A. A. Firsov, *Science*, 2004, **306**, 666–669; (*b*) A. Reina, X. Jia, J. Ho, D. Nezich, H. Son, V. Bulovic, M. S. Dresselhaus and J. Kong, Large Area, *Nano Lett.*, 2009, **9**, 30–35.
4 (*a*) B. C. Brodie, *Ann. Chim. Phys.*, 1860, **59**, 466–472; (*b*) W. S. Hummers and R. E. Offeman, *J. Am. Chem. Soc.*, 1958, **80**, 1339–1340; (*c*) K. S. Novoselov, V. I. Falko, L. Colombo, P. R. Gellert, M. G. Schwab and K. Kim, *Nature*, 2012, **490**, 192–200; (*d*) D. R. Dreyer, S. Park, C. W. Bielawski and R. S. Ruoff, *Chem. Soc. Rev.*, 2010, **39**, 228–240.
5 (*a*) M. Zhou, Y. Wang, Y. Zhai, J. Zhai, W. Ren, F. Wang and S. Dong, *Chem.–Eur. J.*, 2009, **15**, 6116–6120; (*b*) D. Kang and H. S. Shin, *Carbon Lett.*, 2012, **13**, 39–43.
6 S. Mao, H. Pu and J. Chen, *RSC Adv.*, 2012, **2**, 2643–2662.
7 S. Eigler, M. E-Heim, S. Grimm, P. Hofmann, W. Kroener, A. Geworski, C. Dotzer, M. Rockert, J. Xiao, C. Papp, O. Lytken, H.-P. Steinruck, P. Muller and A. Hirsch, *Adv. Mater.*, 2013, **25**, 3583–3587.
8 J. Chen, B. Yao, C. Li and G. Shi, *Carbon*, 2013, **64**, 225–229.
9 (*a*) Y. Kopelevich and P. Esquinazi, *Adv. Mater.*, 2007, **19**, 4559–4563; (*b*) J. Zhao, S. Pei, W. Ren, L. Gao and H.-M. Cheng, *ACS Nano*, 2010, **4**, 5245–5252.
10 (*a*) S. Pei and H.-M. Cheng, *Carbon*, 2012, **50**, 33210–33228; (*b*) S. Y. Toh, K. S. Loh, S. K. Kamarudin and W. R. W. Daud, *Chem. Eng. J.*, 2014, **251**, 422–434; (*c*) C. Liu, F. Hao, X. Zhao, Q. Zhao, S. Luo and H. Lin, *Sci. Rep.*, 2014, **4**, 3965; (*d*) H. Wang, J. T. Robinson, X. Li and H. Dai, *J. Am. Chem. Soc.*, 2009, **131**, 9910–9911; (*e*) T. Kuila, A. K. Mishra, P. Khanra, N. H. Kim and J. H. Lee, *Nanoscale*, 2013, **5**, 52–71.
11 S. Pei and H.-M. Cheng, *Carbon*, 2012, **50**, 3210–3228.

12 (*a*) Y. Hu, S. Song and A. L. Valdivieso, *J. Colloid Interface Sci.*, 2015, **450**, 68–73; (*b*) Y. Xu, K. Sheng, C. Li and G. Shi, *J. Mater. Chem.*, 2011, **21**, 7376–7380.

13 (*a*) R. Kumar, P. Kumar, S. Naqvi, N. Gupta, N. Saxena, J. Gaur, J. K. Maurya and S. Chand, *New J. Chem.*, 2014, **38**, 4922–4930; (*b*) W. Kwon, Y.-H. Kim, C.-L. Lee, M. Lee, H. C. Choi, T.-W. Lee and S.-W. Rhee, *Nano Lett.*, 2014, **14**, 1306–1311.

14 M. Tromel and M. Russ, *Angew. Chem.*, 1987, **99**, 1037–1038.

15 (*a*) D. C. Maracano, D. V. Kosynkin, J. M. Berlin, A. Sinitskii, Z. Sun, A. Slesarev, L. B. Alemany, W. Lu and J. M. Tour, *ACS Nano*, 2010, **4**, 4806–4814; (*b*) Y. Hong, Z. Wang and X. Jin, *Sci. Rep.*, 2013, **3**, 3439.

16 R. Singh and T. H. Goswami, *Thermochim. Acta*, 2011, **513**, 60–67.

17 S. Eigler and A. Hirsch, *Angew. Chem., Int. Ed.*, 2014, **53**, 7720–7738.

18 S. Peterson, Y. He, J. Lang, F. Pizzocchero, N. Bovet, P. Boggild, W. Hu and B. W. Laursen, *Chem. Mater.*, 2013, **25**, 4839–4848.

19 (*a*) F. Banhart, J. Kotakoski and A. V. Krasheninnikov, *ACS Nano*, 2010, **5**, 26–41; (*b*) X. Guangyu, Z. Yuegang, D. Xiangfeng, A. A. Balandin and K. L. Wang, *Proc. IEEE*, 2013, **101**, 1670–1688.

20 F. Tuinstra and J. L. Koenig, *J. Chem. Phys.*, 1970, **53**, 1126–1130.

21 Y. Zhu, S. Murali, W. Cai, X. Li, J. W. Suk, J. R. Potts and R. S. Ruoff, *Adv. Mater.*, 2010, **22**, 3906–3924.

22 H.-J. Shin, K. K. Kim, A. Benayad, S.-M. Yoon, H. K. Park and I.-S. Jung, *Adv. Funct. Mater.*, 2009, **19**, 1987–1992.

